CHALMERS
UNIVERSITY OF TECHNOLOGY

Road Signs as Reference Objects for Autonomous Driving

Master thesis report

Master's thesis in Electrical Engineering

GOWTHAM GUNASHEKARA

DEPARTMENT OF ELECTRICAL ENGINEERING
CHALMERS UNIVERSITY OF TECHNOLOGY
Gothenburg, Sweden 2022
www.chalmers.se

Master's thesis 2022

Road Signs as Reference Objects for Autonomous Driving

Master thesis report

Gowtham Gunasheakara

CHALMERS
UNIVERSITY OF TECHNOLOGY

Department of Electrical Engineering
Division of Automotive Engineering
Chalmers University of Technology
Gothenburg, Sweden 2022

Road signs as reference objects for autonomous driving
Master thesis report
Gowtham Gunashekara

Supervisor: Carl-Henrik Hanquist, Researcher, Measurement Science and Technology, Dimension and Position, RISE
Examiner: Henk Wymeersch, Professor, Communication systems, Dept. of Electrical Engineering

Master's Thesis 2022
Department of Electrical Engineering
Division of Automotive Engineering
Chalmers University of Technology
SE-412 96 Gothenburg
Telephone +46 31 772 1000

Cover: GNSS position measurements performed by Carl-Henrik Hanqvist on Astazero track.

Typeset in LaTeX
Printed by Chalmers Reproservice
Gothenburg, Sweden 2022

Road signs as reference objects for autonomous driving
Gowtham Gunashekara
Department of Electrical Engineering
Chalmers University of Technology

Abstract

One of the significant challenges in the development of autonomous driving is building detailed three dimensional high-definition (HD) maps and keeping them updated. The reasons may be the constant change in road infrastructure or the physical drift of these objects due to the environmental changes (like the frost thaw cycles occurring annually), urban development, or natural phenomena that may occur.

This thesis deals with understanding the stability of road signs over time, or due to the geological changes/weather cycles, etc., and the uncertainty the stability brings to the autonomous driving systems while navigating in the presence of road signs. This project studies road signs, their placement, the current classification methods and tries to devise a new method suitable for the purpose of autonomous driving. Analyses are performed to investigate the possibility of certain classes of road signs addressed as reference objects.

First, the road signs are classified based on stability and mobility, then road sign measurements are recorded using a global navigation satellite system receiver. A stability analysis involves studying the tilt of standard road signs, visualising the data, constructing uncertainty budgets, and drawing conclusions. Then the position data of the custom-made reference object is analysed, and uncertainty budget is constructed. The combined standard measurement uncertainties of the regular and custom-made object are compared to gauge the performance.

After analysing the collected road sign data, it was found out that the road signs are not stable. Out of 27 road signs that were studied, 7 objects were found to be tilted more than 5°. The combined standard measurement uncertainty value for the custom-made object is approximately 20% of that calculated for a regular road sign (worst case). Due to their instability, the regular road signs cannot be used as long-term reference objects. A huge outlier was observed in the visualised SWEREF 99 TM data of the custom object and was attributed to either a bird visit or heavy rainfall. Other outliers may be heavy rain/snowfall, dense clouds in signal path and data data integration errors. The weather, soil and wind effects, long term stability study, incorporation of radomes to prevent obstruction mainly by birds, etc. can be pursued in the future.

Keywords: Autonomous vehicles, Classification, GNSS, High-Definition maps, Measurement uncertainty, Metrology, Reference object, Road signs, Stability.

Acknowledgements

I would like to express my heartfelt appreciation to my supervisor Carl-Henrik Hanquist at RISE for providing me with this exciting opportunity to put my skills into action throughout the project, for his continuous support throughout the project, for widening my perspective and for providing me with continuous feedback of all kinds to help me grow as an individual. I would also like to extend my thanks to Erik Bäckman, who has provided me with all the help he could throughout the project and during the field measurements. Thank you both for providing me with all the guidance and help.

I would also like to thank Jörgen Spetz for hiring me and providing me with this wonderful opportunity to work with some really experienced and talented group of people, and also for a smooth on-boarding experience.

Furthermore, I would like to deeply acknowledge my examiner Henk Wymeersch, for always guiding me throughout the project and Shen Li, for answering all my queries quickly, helping me with all the administrative processes and constantly checking on the thesis work.

I would like to thank Gabriel Jamie Garcia and his team in Zenseact for the autonomous test vehicle which was used throughout the project.

Hearfelt thanks to Adam Eriksson, from Astazero for arranging the track, and for supporting us with all the necessary resources in the premises and the Astazero employees for always helping out when needed, providing us with tools and also for setting up the scenario during every field work session.

Lastly, I would like to extend my gratitude to all my friends and family for guiding, inspiring and constantly supporting me during this entire thesis project.

Gowtham Gunashekara, Gothenburg, August 2022

List of Acronyms

Below is the list of acronyms that have been used throughout this thesis listed in alphabetical order:

ACC	Adaptive Cruise Control
AD	Autonomous Driving
ADAS	Advanced Driver Assistance Systems
AEB	Autonomous Emergency Braking
BOW	Bag Of Words
CV	Connected Vehicles
E-tolls	Electronic Tolls
ETRS89	European Terrestrial Reference System 1989
GNSS	Global Navigation Satellite System
GIS	Geographic Information Systems
GPS	Global Positioning System
HD Maps	High-definition Maps
IGS	International GNSS Service
I2V	Infrastructure To Vehicle communication
LIDAR	Light Detection And Ranging
LTE	Long Term Evolution
MATLAB	Matrix Laboratory, Software
NGK2015	Nordic Geodetic Commission (quasi)geoid model
N-RTK	Network Real-Time Kinematic
PPK	Post Processed Kinematic
PPP	Precise Point Positioning
RADAR	Radio Detection And Ranging
RTK	Real-Time Kinematic
SAE	Society of Automotive Engineers
SWEREF 99 TM	Swedish Reference Frame 1999 National Map Projection
UNC	Unified National Coarse Thread
V2X	Vehicle To Everything (I - Infrastructure, V - Vehicles, etc.) communication
WGS	World Geodetic System

Nomenclature

Below is the nomenclature of parameters and variables that have been used throughout this thesis.

Symbols used

$X_0, X_1, ..., X_n$	Factors of the budget
$x_0, x_1, ..., x_n$	Estimated value of the factors
$u(x_i)$	Standard uncertainties
c_i	Sensitivity co-efficient
d	Divisor
$d1$	Distance between road sign base and sign centre (m)
d_{prevent}	Known prevention distance (m)
d_{roadwork}	Distance of roadwork (m)
$h1$	Measured pole height (m)
$u_i(y)$	Standard measurement uncertainty
$u(y)$	Total measurement uncertainty (m)
ΔL	change in length of object (m)
θ	Angle of tilt (rad)
μ	Mean value of the distribution
σ	Standard deviation value of the distribution
α	thermal expansion co-efficient (K^{-1})

Contents

List of Figures

List of Tables

1
Introduction

This section explains the problem in focus, the research performed in the field and the objectives aimed to reach in this project and the approach used to achieve the goals.

1.1 Problem description

Autonomous and connected vehicles are the future of road transportation. Research is being conducted in these fields to streamline and organise the traffic flow efficiently. In order to realise a high level of autonomy in vehicles, sensor information such as GPS, LIDAR, camera image data regarding the vehicle's surroundings is of highest importance [2]. HD maps are important to help position a vehicle with a high level of accuracy on the lane/road and to build safe, fast driving routes based on the upcoming traffic and surroundings data [3]. Therefore, HD maps also in a way act as sensors, and hence must always be up-to-date with plethora of information [4]. Establishing clear communication channels between the vehicles (vehicle-to-vehicle communication), and between vehicles and the road infrastructure (vehicle-to-infrastructure communication) is important. Also, sensor information exchange should occur flawlessly to facilitate updation of the HD maps continuously.

This project involves such HD maps with information regarding road sgins which can potentially be used as references for autonomous driving. A potential problem with using roadside infrastructure as reference is their stability and the effects that may have on the autonomous vehicles.

Not just improved sensors, but improved road infrastructure and clearly defined traffic rules are also essential to make autonomous vehicles a reality. In 2018, an investigation was conducted in this regard. Some of the topics explored involved were definition of lanes, markings, introduction of new road signs for autonomous vehicle lanes, rules, permits, etc. [5].

1.2 Aim and objectives

The purpose of this research is to understand the nature of roadside such as barriers, road signs, lane markings, their stability, and selection of objects which can potentially act as reference points for autonomous driving. There are classifications of the road-signs based on various factors such as type, shape, colour, etc. [6, 7, 8],

based on many artificial intelligence techniques such as neural networks and image processing techniques. There are classifications based on the type of sign (warning, prohibitory, special, etc.), but none of them take the sign stability into account. Hence, in this thesis, a study is conducted to determine if there is a more relevant classification method for the purpose. Uncertainty analyses will be performed to obtain information regarding the extent to which the factors affect the measurements and the object stability. A custom made object is also included in the study in order to assess its performance in comparison with the standard roadside object so that it can be utilized as a reference in HD maps in the future.

1.3 Scientific Approach

First, the various kinds of roadside objects, their structural stability, the types of foundations, placement methods, and the maintenance are studied. Next, detection methods for these objects are studied along with the types of classification. Then, physical inspection of road signs and observations are done in order to get a clear picture of the real life stability of these objects. A set of measurements are then performed on road signs to evaluate their stability. The physical dimensions of the objects, the surface on which the object is placed, the amount of motion in various directions from application of a small physical force (simple pushing or tugging), etc., are noted.

Later, an uncertainty analysis is performed. The factors which may have introduced an error in the measurement are noted down, and based on prior experience and observations, they are categorised and the extent of their effect is estimated. An uncertainty budget is then built to understand the extent of influence of these factors on the combined measurement uncertainty and how they can be controlled. The budget provides insights regarding the direction in which there is scope for improvement to obtain a smaller uncertainty, and hence increasing the reliability of the road sign as a potential reference object.

Once the measurements are performed on multiple objects, the results obtained are visualised and analysed using MATLAB.

2
Theory

This section explains the concepts needed to understand the thesis work. It contains the basic concepts of metrology and measurement uncertainty to understand the analyses performed. It provides a small overview of HD maps and the amount of useful information it contains. Autonomous driving and connected cars are ways to reduce crashes and help achieve safer roads for users. The positioning requirements demanded by ADAS and CV systems that can help achieve certain degree of safety and autonomy are explained briefly. The various GNSS techniques employed by receivers are explained to help choose the right one for the set purpose. Some light is also thrown upon the co-ordinate systems used, both in Sweden and other countries for positioning and mapping.

2.1 Metrology

Measurement is defined as the "*process of experimentally obtaining one or more quantity values that can reasonably be attributed to a quantity*" [9]. Measurand is nothing but the quantity that needs to be expressed in a magnitude.

Metrology is the science of such measurement. "Metrology" is derived from the Greek word "Metro" which means measure. It includes all kinds of measurements such as mass, length, time, etc. Measurements are an important part of daily life, and metrology standardises the process by clearly defining the quantities of measures (both standard and derived), their conversions and so on. According to the International organisation of legal metrology, "*Metrology involves both the theoertical and practical aspect of measurement, irrespective of the measurement uncertainty or the field of application*" [10].

Legal metrology is a seperate section in metrology which sets the legal requirements, keeps track of the standards of the measurements and the measurement devices. It also makes sure that manufacturers comply to the standards while mass producing or exporting these devices. It is also in charge of assessing the regulated devices and measurements carried out using the same. It is also useful for the traceability of such measurements and devices back to international standards [10].

2.2 Measurement uncertainty

Measurement uncertainty is a non-negative value which defines the range of variation of the quantity values of the measurand [9]. It helps quantify the amount of error in any measurement. An example of the standard method of specifying length is

$$\text{length} = 10.02 \pm 0.05 \text{ m}, \tag{2.1}$$

where 10.02 m is the **quantity value** arrived at, after measuring 10.019123453123 m, building an uncertainty budget and arriving at a measurement uncertainty of $\pm$ 0.05 m.

Measurements can be influenced by a multitude of factors. Fig. 2.1 represents some of the sources of uncertainty.

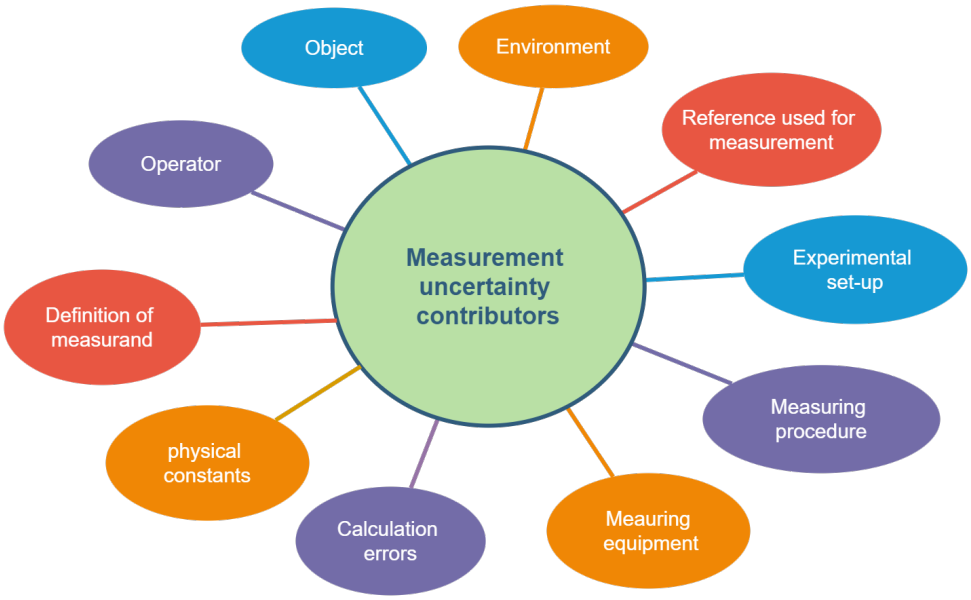

Figure 2.1: A diagram showing the factors that influence the measurement uncertainty.

Measurement uncertainty analysis is a process of identifying all the various factors contributing to the error and gauging the size of their contributions. It is performed by creating an uncertainty budget, which gives a rough idea of the effect of the contributors on the measurement. A typical uncertainty budget is shown in Table 2.1. As the budget becomes more complicated, it can provide very accurate details on what affects the uncertainty. The uncertainty budget helps identify the main contributors affecting the uncertainty, and metrologists usually try to work on these by making changes in the measurement procedure, technique or equipment, by bringing about changes in the measured object and so on.

The evaluation of measurement uncertainty is generally carried out in one of the two ways [9]:

Type A: A series of measurements are taken and its standard deviation is identified. Based on the quantity value's statistical distribution, it is evaluated systematically.
Type B: Based on prior experience and knowledge, the quantity values are represented in the form of a probability density function. Additionally, it can also be represented as a statistical distribution and then evaluation is performed on it.

The measurement whose uncertainty is to be evaluated is the first member of the budget. The list of factors affecting the uncertainty occupy the subsequent rows of the budget.

Indexing from 0: First, a symbol is assigned to each of the elements of the budget (X_0, X_1,....., X_n). Then, the estimated values for each factor are noted down (represented by x_0, x_1,...., x_n). Next, each factor is represented in terms of a probability distribution which can represent it reasonably. Later, the amount of error each factor gives is evaluated. Then, all the estimated uncertainties are converted into standard uncertainties $u(x_i)$ by means of a divisor d. The equation for conversion is

$$u(x_i) = \frac{x_i}{d}, \tag{2.2}$$

where $d = \sqrt{3}$ for rectangular distribution, $\sqrt{6}$ for triangular distribution and 1 for normal distribution

Next, the sensitivity coefficient c_i is evaluated for each of the factors. It describes the degree of effect it has on the output when there are changes in the input [9]. It also helps bring all the factors to a standard unit in order to ease the next step. Then, the contributions $u_i(y)$ of the factor to the overall measurement uncertainty is calculated using the equation:

$$u_i(y) = c_i \cdot u(x_i). \tag{2.3}$$

The total measurement uncertainty $u(y)$ is the quadratic sum of all the uncertainties $u_i(y)$ that are obtained due to the various factors influencing it, which is given by:

$$u(y) = \sqrt{\sum_{i=1}^{n} u_i(y)^2} = \sqrt{u_1(y)^2 + u_2(y)^2 + ... + u_n(y)^2} \tag{2.4}$$

Quantity	**Estimated value**	**Unit**	**Proabability distribution**	**Standard uncertainty**	**Sensitivity co-effiecient**	**Unit**	**Contribution**
X_1	x_1	cm	distribution 1	$u(x_1)$	c_1	m	$u_1(y)$
X_2	x_2	mm	distribution 2	$u(x_2)$	c_2	m	$u_2(y)$
.	.	.	.	.	.	.	.
.	.	.	.	.	.	.	.
X_n	x_n	dm	distribution n	$u(x_n)$	c_n	m	$u_n(y)$
							$u(y)$

Table 2.1: Typical uncertainty budget

2.3 Autonomous driving

Transport safety is one of the top priorities of vehicle manufacturers and governments across the globe. According to the article [11] published by the European commission, there has been a 36% reduce in the number of traffic fatalities in the last decade in Europe. The parliament is working continuously and introducing new regulations in order to further reduce this number. One such strategy is **Vision Zero**. First introduced in Sweden, it aims to reduce the number of deaths/serious injuries related to traffic to zero. This strategy has slowly been adapted by the entire European union and is now creeping to the USA [12].

Human error, fatigue and stress are the main reasons for traffic accidents. In order to tackle this problem, researchers are working hard towards making the dream of autonomous vehicles a reality, while developing systems which aid the driver when they get into a safety critical situation. Advanced/autonomous driver-assistance systems (ADAS) have become an integral part of vehicles these days. It aims at achieving some level of vehicle safety and autonomy. ADAS systems employ a range of sensors such as global navigation satellite systems (GNSS), light/radio detection and ranging (LIDARs/Radars), cameras, laser scanners, etc, and sometimes collect data from multiple sensors in order to actively take better traffic safety decisions [2]. These systems also use the data obtained from the communication between the ego vehicle and other sources (V2X communication) to assess the position of the ego relative to the vehicles and the road traffic infrastructure surrounding it. The communication between traffic members for the purpose of safety, improved traffic management and mobility is called connected vehicle (CV) technology [1].

Positioning requirements for CV and ADAS systems are of four types [1]:

- **None**: There is no positioning requirement. Eg: E-tolls.
- **Where-on-road**: a coarse position of the vehicle and the part of road it is travelling on. Position accuracy: 5-10 metres. Eg: Speed limit warning, etc.
- **Where-in-road**: a more accurate positioning to indicate the lane in which the vehicle is driving. Position accuracy: less than 1 m. Eg: speed warning at curves, blind-spot warning, etc.
- **Where-in-lane**: highly accurate positioning to indicate the position of the vehicle within a lane. Position accuracy: less than 10 cm. Eg: Lane departure warning, forward collision warning, etc.

Some examples for ADAS systems would be forward collision warning, lane departure warning, adaptive cruise control, etc. Some of these systems aid the driver to have a safer driving experience by either warning them when they are approaching a safety critical situation, or taking control of the driving task (worst case), whereas others try to reduce the stress involved in the driving task and enable them to relax and perform a secondary task.

Autonomous vehicles integrate an array of sensors that sense the driving environment with computing power which makes smart traffic related decisions (using machine learning and artificial intelligence) and provides input to the vehicle control systems in order to complete the driving task safely without human aid/interference.

The society of automotive engineers (SAE) has defined the various levels of autonomy in vehicles. Table 2.2 briefly explains the levels.

Number	Automation level	Definition
0	Manual control (No Automation)	- Driver performs all the tasks involved in driving.
1	Driver assistance	- Vehicle contains a simple system. - Assistance with one of the driving tasks like steering, braking or acceleration. E.g.: Cruise control.
2	Partial automation	- The vehicle consists of ADAS systems such as ACC and AEB. - Can perform the basic driving tasks. - Driver must monitor these systems and can take over control any time.
3	Conditional automation	- The vehicle can perform all the driving tasks automatically only in certain cases. - Driver will have to intervene in certain cases.
4	High automation	- The vehicle will perform the all the driving tasks under certain conditions. - Requires the exact position of the vehicle with reference to the road (where-in-lane level). - Optional driver intervention capabilities.
5	Full automation	- The vehicle will perform all the driving tasks under all conditions. - Human monitoring is not needed. - Driver can perform secondary tasks.

Table 2.2: SAE levels of automation [1].

2.4 HD Maps

Autonomous vehicles are ones which can perform the driving task on their own, with the aid of sensors, processing power and actuators. HD maps are high precision maps with multiple layers consisting of the latest information (geometric information of the road, its infrastructure and the environment around it) [13].

HD maps are unlike regular maps. Most information is stored on cloud, and only the information needed is rendered to reduce the load on the computer in the vehicle. HD map layers consist of massive amounts of data like the types of surfaces, height of various objects on the road, lane information like shape, size, direction, mark-

ings, type, lane connections, and the various restrictions that apply to the various roads/lanes, traffic signals, road-signs, dividers, barriers, etc [13].

2.5 GNSS receivers

GNSS sensors are one of the most important positioning sensors in an autonomous vehicle. GNSS satellites are a cluster of satellites which provide L-band signals (with frequency range 1000-1700 MHz [14]) consisting of ranging codes and navigation information to the receivers, allowing them to calculate their geological position. GNSS positioning accuracy can vary from a few metres to just a few centimetres. There are many clusters of GNSS satellites such as GPS (USA), GLONASS (Russia), Galileo (Europe), etc. There are different techniques employed in GNSS such as real-time kinematic (RTK), post-processed kinematic (PPK), precision point positioning (PPP) and network-RTK.

RTK: This technique involves two receivers. A base station and a rover. The position of a base station is established. When it receives signals from the GNSS satellites, it calculates the error between the received signal and the position data already available, and then transmits this information to the receiving rover, so that position correction can be performed in real-time.

N-RTK: Similar to RTK technique, this technique uses a network infrastructure to receive position data from a few satellites in the cluster and send this to the base station for processing of correction data. The final correction data is sent to the rover through networks. This technique may require much less numbers of satellites from the cluster to begin operation, and there is no need to set up a base station by oneself.

PPK: This technique does not employ real-time communications between the base station and the rover. Rover collect the position data and the base station collects position data with a much higher accuracy. The correction is later performed in the post-processing step.

PPP: In this technique, only one receiver is used (the rover). It collects the raw positioning data from the GNSS satellites, and relies on receiving measurements of GNSS satellite orbit from organisations such as IGS [15] for correction of the raw data in order to calculate the position with a much higher accuracy.

For this project, N-RTK GNSS receiver was used for the field work. This technique employs computational complexity lesser than the other methods, since there is a link with a nearby base station to receive real-time correction signals at all times. The anchor point (custom-made reference object) employs a PPK system since it's a stationary object whose purpose is to be simple yet functional.

2.6 Driving scenarios

For this project, three different driving hazard scenarios have been designed in order to validate the HD maps and confirm if the localization of the vehicle is occurring successfully. All the scenarios involve a roadwork with 2 road-signs, and all the images representing the scenarios are obtained, courtesy of Zenseact.

2.6.1 Scenario 1

The first warning road-sign is at a known distance of $d_{\text{prevent}} = 1000$ m from the roadwork. The second one is at the start of roadwork. There are solid yellow lane markings on both sides of the lane to signify the length of roadwork. The roadwork length d_{roadwork} is variable during each test run. Fig. 2.2 shows the scenario implemented on the track.

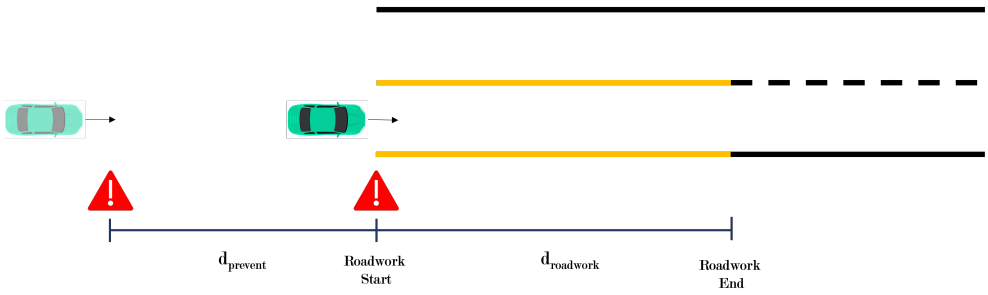

Figure 2.2: Roadwork scenario 1

2.6.2 Scenario 2

The positions of the warning signs are the same as scenario 1, but here the yellow lane markers are absent. Instead, the regular white lane markings are present on one side. Fig. 2.3 shows the scenario implemented on the track.

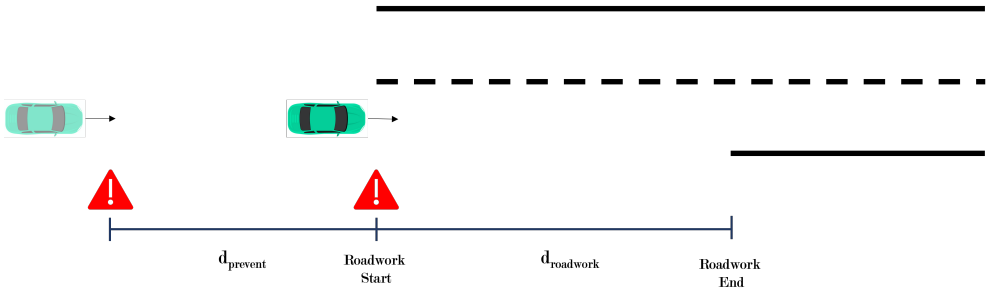

Figure 2.3: Roadwork scenario 2

2.6.3 Scenario 3

The positions of the warning signs are the same as scenario 1, but this case involves a two-lane road converging to a single lane road, signified by the presence of yellow road markers in between the two lanes as shown in Fig. 2.4.

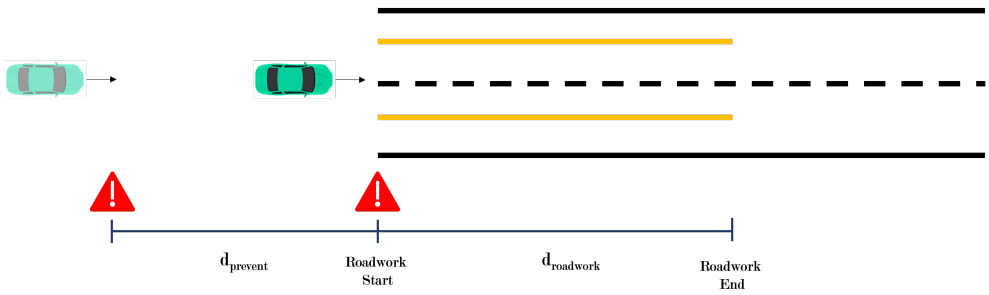

Figure 2.4: Roadwork scenario 3

2.7 Co-ordinate systems

There are different co-ordinates systems used by different organisations in different parts of the world for mapping, surveying, and navigating. Explained below are the ones used in this research.

2.7.1 WGS 84

WGS 84 is a standard co-ordinate system developed by the USA used as a reference by GPS satellites. It is also called earth-centred, earth-fixed (ECEF) terrestrial co-ordinate system with its origin at the centre of mass of the planet [16]. It is based on an ellipsoid (called WGS 84 ellipsoid) which acts as a reference datum for measurements over the sea level. WGS 84 co-ordinates are of the form x, y and z co-ordinates.

This co-ordinate system got updated over the years in order to align well with the changes occurring on Earth due to the planetary motion and the tectonic activities. It is a very reliable reference frame which rotates with the earth and is widely used in geodesy, mapping, surveying, and so on worldwide.

2.7.2 SWEREF 99

SWEREF 99 is a three-dimensional (3D) reference system, which stands for “Swedish reference frame 1999”. It is similar to the WGS 84 and can be used as a reliable alternative. The difference between them is in the decimeter level (7-8 dm) as of 2021 [17]. It is based on the European reference system ETRS89, and is widely used in positioning, geodesy, and other purposes throughout Sweden.

This reference system is realised by the support of 21 permanent swepos stations in Sweden and also by other stations in the surrounding Scandinavian countries. It

is continuously updated to keep up with the changes in the geoid due to tectonic movements.

2.7.3 SWEREF 99 TM

SWEREF 99 TM is a map projection system based on the SWEREF 99 reference system which is used for most technical applications (mapping and land surveying) in Sweden [18]. It is more practical for the purpose compared to 3D or latitude longitude co-ordinate systems. This co-ordinate system has 2 components, Northing (N) measured from the equator (zero point) to the North pole, Easting (E) measured from the central meridian (zero point) and increases with distance in the east direction.

Sweden uses the 15° meridian as the reference (E) and equator as the origin (N). For this thesis, all the co-ordinates measured were in SWEREF 99 TM format.

2.7.4 SWEN17_RH2000

In the hunt for realizing better geoid models, SWEN17_RH2000 was built. NGK2015 is the gravimetric model which is the basis of this system. This system has been established by the Nordic commission of geodesy (NKG) in a Nordic/Baltic cooperation [19].

The system RH2000 provides the height above sea level (H) component to give the elevation for the points measured using SWEREF 99 TM.

2.8 Summary

Transport safety is one of the important fields of research in the automotive industry. There are many warning and autonomous systems which help a driver avoid crashes in an unexpected situation, and every system has its set of positioning requirements to deliver efficient performance. Autonomous driving and connected cars can help ease the pressure on the driving task and can encourage the user to perform secondary tasks. GNSS employs many techniques, but for this thesis, the measurement pole employed an N-RTK receiver to reduce computational power used and the anchor point employed a PPK receiver, since it is a stationary object whose weight was needed to be kept as low as possible to avoid deformation of the truss mast in any direction, which may influence the GNSS position of the object. The co-ordinate system used in Sweden for 2D mapping is called SWEREF 99 TM, and the third dimension (the height above the sea level) is provided by the SWEN17_RH2000. The system is similar to WGS 84 ECEF co-ordinate system.

3
Methods

This section goes through the design of the custom-made reference object, its components and the GNSS data collection set up mounted on it. It is a truss mast structure on a concrete foundation, with a top plate and a three armed sign holder. It also has the provision to mount magnetic ball base on which reflecting prisms can be placed to perform measurements using laser scanners in the future. It is mounted with a multi-constellation GNSS receiver setup with a modem and antenna for data collection. Next, the road signs are classified into three major classes based on their stability. The custom-made reference object stability analysis is performed. Later, the list of measurements taken is explained along with the equipment used. The measurements obtained are cleaned, and co-ordinates are verified using GIS tools such as Google Earth. The data is then imported into MATLAB where calculations are performed to determine the pole tilts for the 27 road signs measured. After this, the uncertainty factors are determined and accounted in the uncertainty budget.

3.1 Custom-made reference object

The custom-made reference object is designed to be a high grade anchor point. The focus of this design was for it to be a trustworthy one and also to serve multiple purposes, such as being a test object for position validation, algorithm verification for HD map updates, and sensor performance evaluation. The resulting design was aimed to achieve good performance. The object consists of four main parts, a concrete foundation, a truss mast, a top-plate, and an arm with a road sign.

The dimensions of the concrete fundament (foundation) are $1300 \times 1300 \times 500$ mm. The truss mast projects to height of 3000 mm and each side is of width 380 mm. The truss mast is equipped with four centering plates (as shown in Fig. 3.2(b)) welded onto the four edges to install magnetic ball base on which reflective prisms are mounted for geodetic measurement using total stations. Fig. 3.1 gives the schematic of the concrete base and the truss mast.

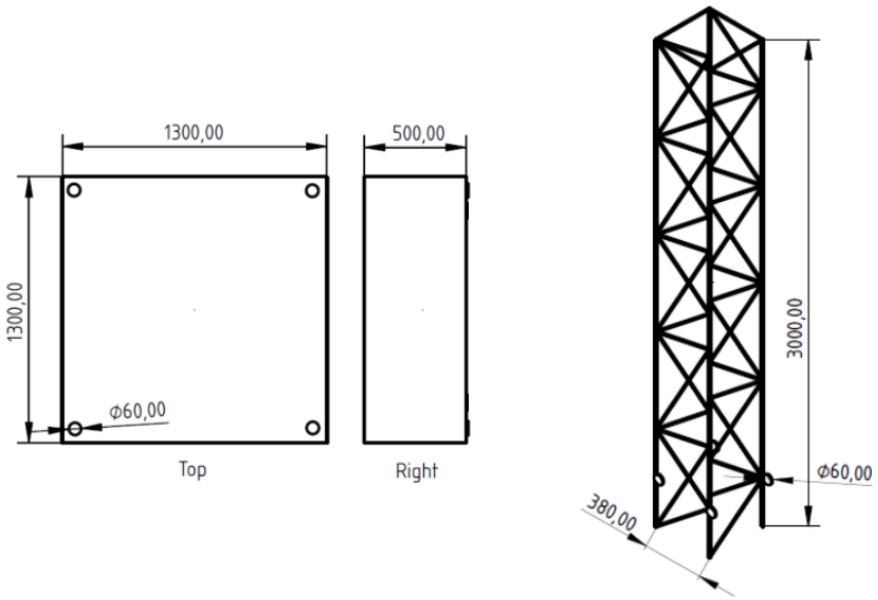

Figure 3.1: Initial drawings of the custom-made object's concrete fundament (left) and the truss mast (right).

Figure 3.2: Truss mast standing on ground with speed limit sign mounted (left) and mounts for the magnetic ball base to place reflecting prisms for laser scanner measurements(right).

A three armed sign holder is mounted on the truss mast, extending perpendicular to the mast, pointing towards the road. The dimensions and schematics of the arm is shown in Fig. 3.3. A circular speed limit sign of 300 mm radius and 10 mm thickness is fixed on the arm as shown in Fig. 3.2

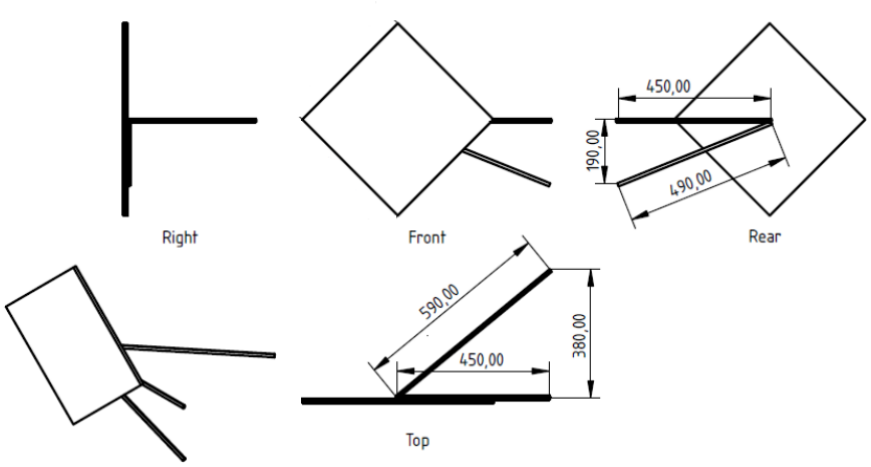

Figure 3.3: Initial drawings of the three armed sign holder.

Figure 3.4: Measurement points on the concrete base and top plate of the custom-made object.

The blue circles in Fig. 3.4 represent the corner points of the base where GNSS position measurements are taken (reference points). Similarly, the top plate has circular centering plates welded on each of the four corners to install a magnetic ball base similar to the truss mast. The points are marked by red circles in Fig. 3.2(b).

The top plate is equipped with a UNC bolt of (5/8) inches, on which the GNSS antenna can be mounted. The Leica AS11 multifrequency GNSS antenna is used for this reference station.

The multi-constellation receiver which can receive signals from all the current GNSS constellations is present in a cabinet mounted on the mast, a metal cabinet is mounted (Fig. 3.5) in which the rest of the equipment is stored. The modem used for communication and internet connectivity is a Teltonika TRB140, which is a compact industry grade, energy efficient system that supports LTE and consists of standard I/O ports. The reference station/anchor point after the components are mounted is shown in Fig 3.6.

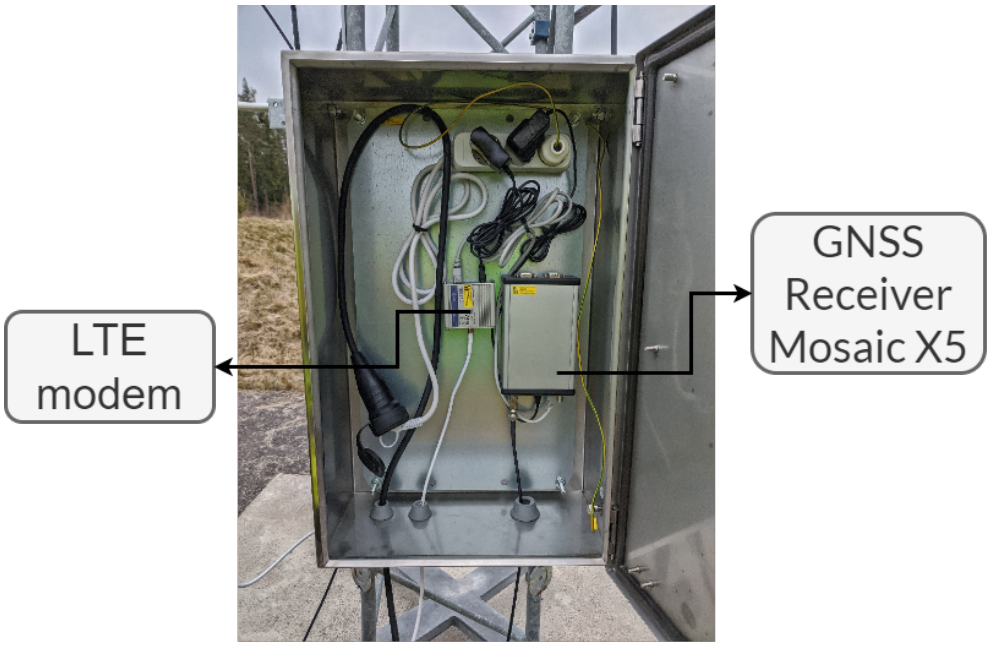

Figure 3.5: The box mounted on the side of the truss mast containing the power supply and the modem.

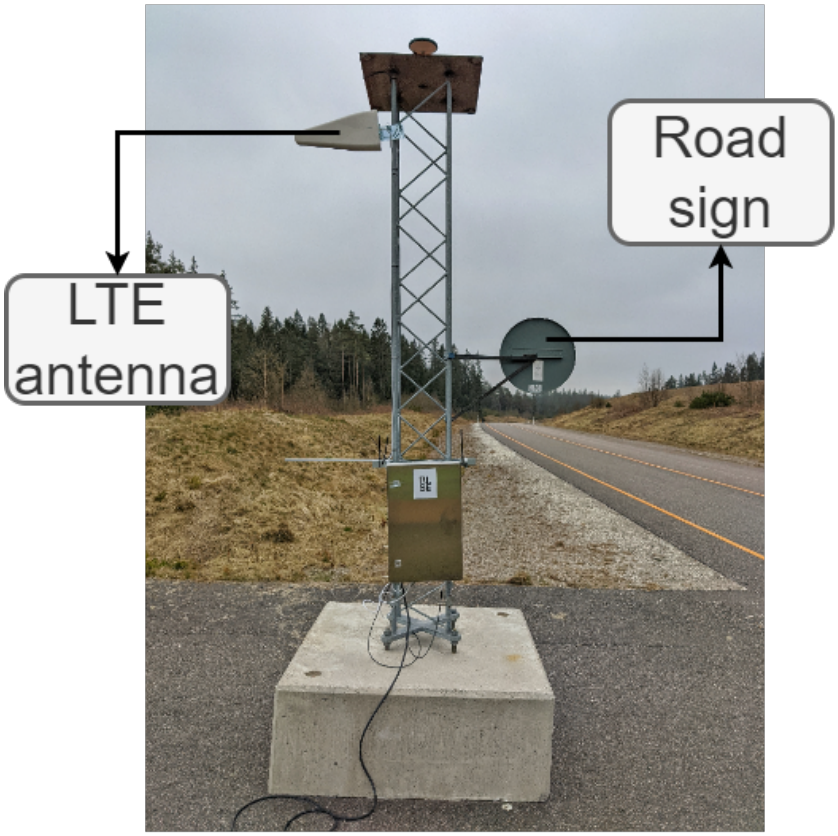

Figure 3.6: Reference station after being set up and components mounted.

3.2 Classification of road signs

The first step was to conduct literature review regarding the existing classifications of road signs. After extensive reading, it was found that the road signs have been classified based on their colours, shapes, or types (warning, information, hazard, etc.). Some of the methods used for this classification are stereo vision [20], bag of words (BOW) [21], artificial neural networks [22, 23], support-vector machines [24], etc. There have been studies conducted regarding the stability of overhead cantilever supports holding road signs in highways [25], concrete footing shape and its settlement characteristics [26] and so on, but there is not much work in the direction of stability of the road signs, nor the standards of their fundament (concrete foot).

A lot of effort was put into contacting governing bodies and companies which supply the road signs to the government regarding the same, but none responded positively. This resulted in building a fresh classification based on experience and observations. Table 3.1 is the classification of the road side objects:

Class		**Object**	**Positioning over time** 2σ **(95%)**
1	A	Concrete reference object on bedrock	< 10 mm
	B	Pillar/mast on bedrock	15 - 30 mm
2	A	Pillar/mast on concrete fundament	20 - 50 mm
	B	Guard rails	30 - ? mm
	C	Road sign	30 - 80 mm
	D	Reflective poles	30 - ? mm
3	A	Mobile road signs	30 - ? mm
	B	Traffic cones, etc.	50 - ? mm

Table 3.1: Road infrastructure classification in the earlier stage of the project

Class 1: Very good short-term stability and stable in the long run. These object can be used as long-term reference objects and to build N-RTK GNSS reference stations of high stability.

Class 2: Everyday road infrastructure objects. These are designed only for a limited stability, and can move to some degree over time. They can be directly placed on the road surface, or can be buried in the soil, held firmly by gravel. They can be easily moved or destroyed by passing vehicles, extreme weather or human interference.

Class 3: Good short-term stability, but since they are mobile, they cannot be used as long-term reference objects. They are not so heavy, and small amounts of force can change their position. They can be used as anchor points, but not as permanent reference points.

3.3 Field measurements of road signs

Field sessions were conducted and a series of road sign measurements were taken.

The different quantities that were measured were the height of the pole, the GNSS position of the sign pole base, the approximate projection of the centre of the road sign on the ground, the size of the sign, its shape, and the amount of oscillatory motion it experiences in each direction when a small physical force is applied by hand. The tools used for measurements are shown in Fig. 3.7 and are listed below.

- a brass plumb,
- a folding rule,
- an environment logger,
- Leica CS30 windows tablet,
- a N-RTK GNSS land surveyor (Leica GS11) and
- a standard 2 m Leica measurement pole.

These measurements were performed in order to determine the tilt of the sign poles used in the track and perform uncertainty analyses on them.

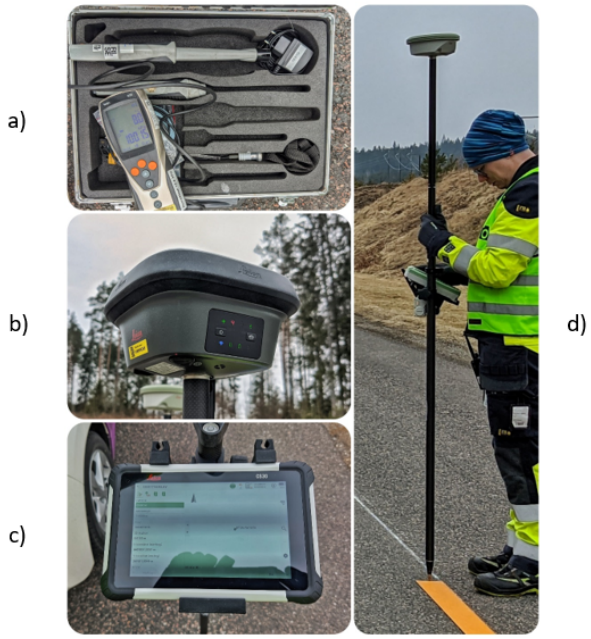

Figure 3.7: (a) The environment logger, (b) Leica GS11 N-RTK GNSS land surveyor, (c) Leica CS30 windows tablet and (d) a Leica standard 2 m measuring pole.

3.4 Data analysis and visualisation

The text file is imported into Excel where it is cleaned up and organised before it can be visualised. After the cleanup, the co-ordinates are plotted in GIS tools such as Google Earth to make sure the measurements are relevant. Later, the data is visualised in various forms and calculations are performed on the measurements to determine the tilt angle in degrees. This information is later used in the uncertainty analysis. A simple sketch supporting the calculation is shown in Fig. 3.8.

Figure 3.8: Measurement being undertaken on road sign number 9, where h1 is the measured pole height (m), d1 is the distance between sign base and sign centre (m) and θ is the angle of tilt (rad).

3.5 Uncertainty analysis

A list of factors that may affect the measurement uncertainty are noted down. The units of measurement are maintained uniformly to simplify the analysis, unless it cannot be avoided. An example uncertainty analysis for the road sign with worst case tilt is given below:

3.5.1 The measurand X_0

In this case, the tilt of the road sign is the measurand, and a list of factors which may affect the measurement uncertainty are listed and their uncertainty is estimated by using prior knowledge or by measurement experience.

When the tilt was measured, the measurement device (GNSS pole) was placed on the ground under the sign, approximately at the centre of the sign. The measurement point was identified with the naked eye. The wind blowing on the sign pushes or shakes it a little and this makes it harder for the eyes to exactly pinpoint the centre of the sign pole. this can cause errors. The contribution is identified as the maximum error and hence a rectangular distribution has been used.

3.5.2 The GNSS quality factor X_1

The device provides this factor, signifying the margin of error based on the number of satellites. usually the factor is below 2 cm, but can increase if the receiver is not able to communicate with satellites as usual.

Since it is the worst case, the same value as the quality factor has been used as the uncertainty. A normal distribution is used as 20-30 measurements were made and the average was obtained, and it is observed that the values are clustered around this average.

3.5.3 The error along sign plane X_2

This factor occurs when the person performing measurements tries to use the plumb to project the sign centre on the ground and tries to place the measurement pole at that exact position in transverse direction. Sometimes the pole cannot be placed directly under the sign due to space constraints or an uneven surface on the floor.

A rectangular distribution is used as there is equal probability of any value between 0 and estimated uncertainty can occur during measurement.

3.5.4 The error perpendicular to sign plane X_3

This factor is similar to the previous one, but considers the error of pole placement in longitudinal direction.

This factor is also assigned a rectangular probability distribution.

3.5.5 The GNSS pole height X_4

The GNSS pole is 200 cm tall with a locking mechanism. Sometimes the locking mechanism can give a small error of up to ± 0.5 cm inclusive of potential bending/-torsional effects, thermal expansion, tip errors, etc.

The distribution used is rectangular, since none of the values within the range have a higher probability of occurrence than the other.

3.5.6 The plumb stability error X_5

The plumb stability error is to evaluate the uncertainty caused by the small circular motion of the plumb that remains despite the effort to hold the string stable. Even after giving it some time, the plumb tends to move due to wind and other factors.

A rectangular distribution is assigned.

3.5.7 The centre positioning error X_6

The centre positioning error is to assess the uncertainty when a human is trying to identify exactly the centre of the sign, then place the plumb string at that point and wait till the plumb stabilises. Sometimes the pole is very tall, and a metrologist trying to reach the sign centre may move his hand a little due to fatigue.

Since the error is random, equal probability is given to all the values within the range, and hence a rectangular distribution is utilized.

3.5.8 The folding scale resolution error X_7

The folding scale resolution is 1 mm, and this term is used to account for the small error that may arise due to the minute resolution of the scale which sometimes can be misread by the human eye. This factor was included to see how much of an impact it can have on the combined uncertainty.

A rectangular distribution is used for this as the probability of reading a value to be lesser/greater than actual are equal.

3.5.9 Folding scale measurement error X_8

When a small force is applied on the pole to shake it and observe the distance to which it oscillates, the folding rule is used. It was just placed a few millimeters away from the pole. Since the oscillation frequency is high, and the folding rule was just floating in the air, there can be errors in determining the distance it moved by the naked eye.

A rectangular distribution is defined due to reasons similar to the previous one.

3.5.10 The object instability error X_9

Generally, the sign poles are placed in the soil, where its fundament is buried in the soil. The stability of the poles are not great. They can rock in multiple directions even with small amount of winds. Hence, when a metrologist is attempting to hold the plumb at the centre of the road sign which is mounted on a pole which is 1.5 - 2.5 m tall, the sign pole might tip a little. It is hard to specify one direction as its resting position.

A rectangular distribution was assigned for this since it was observed that poles are equally unstable in all directions on a 2D plane.

3.5.11 The sign pole edge to sign offset X_{10}

This factor accounts for the error that occurs when determining the distance between the edge of the sign pole to the centre of the plane of the sign. Since the sign poles are tall, and the sign is mounted at a height greater than or equal to the average human height, sometimes there is a possibility of obtaining errors in the measurement due to parallax error and other factors.

A rectangular distribution is utilized for this factor as there was no skew observed when the measurement was repeated.

3.5.12 The pole centre to measurement point error X_{11}

This factor arises due to the fact that there is no fixed point on the pole's edge that is defined to place the measurement pole and conduct the measurements every time. Sometimes the pole does not sit right at the edge and needs some space to stand upright for a few seconds in order to perform measurements.

Since the measurement pole placement is random, and there is no observable trend is the values, a rectangular distribution is assigned to this.

3.5.13 Uncertainty budget

Initially the pole height was assumed to be approximately 3 m. This assumption was based on a picture taken while performing measurements of the most tilted sign with a 2 m pole which can bee seen in Fig. 3.8. Then the pole height for the other objects was assumed to be 2.2 m, which is the standard height of a pole holding a single road sign on a flat road in Sweden [27].

In the later stages, the actual height of the pole from the base to the bottom end of the road sign and the height from bottom of the sign to centre of the sign were measured, and incorporated in the tilt calculation. Table 3.2 shows an uncertainty analysis performed on a sign pole with very high tilt. The sensitivity factor is taken to be 0.01 to convert all the units from centimetres to metres.

Contributor	Symbol X_i	Estimated value x_i	unit1	estimated uncertainty	unit2	Probability distribution	divisor	Standard uncertainty $u(x_i)$	sensitivity coefficient c_i	contribution $c_i \cdot u(x_i)$	unit3	contribution (%)
Tilt	X_0	152.1527	cm	12.5	cm	Rect - R	1.732	7.21709	0.01	0.072171	m	44%
GNSS quality factor	X_1	1.5	cm	1.5	cm	Normal	1	1.5	0.01	0.015	m	2%
Tilt error along the sign plane (transverse)	X_2	0	cm	8	cm	R	1.732	4.618938	0.01	0.046189	m	18%
Tilt error perpendicular to the sign plane (longitudinal)	X_3	0	cm	8	cm	R	1.732	4.618938	0.01	0.046189	m	18%
GNSS pole height	X_4	200	cm	1	cm	R	1.732	0.577367	0.01	0.005774	m	0%
Plumb stability error	X_5	0	cm	2.5	cm	R	1.732	1.443418	0.01	0.014434	m	2%
Centre positioning error (human)	X_6	0	cm	3	cm	R	1.732	1.732102	0.01	0.017321	m	3%
Folding scale resolution	X_7	0.1	cm	0.05	cm	R	1.732	0.028868	0.01	0.000289	m	0%
Folding scale measurement error	X_8	0	cm	2	cm	R	1.732	1.154734	0.01	0.011547	m	1%
Object instability error	X_9	0	cm	5	cm	R	1.732	2.886836	0.01	0.028868	m	7%
Pole edge to sign offset	X_{10}	0	cm	4	cm	R	1.732	2.309469	0.01	0.023095	m	5%
Pole centre to measurement point	X_{11}	2.5	cm	0.5	cm	R	1.732	0.288684	0.01	0.014434	m	2%
									combined standard measurement uncertainty u_c	**0.109320**		**100%**

Table 3.2: Uncertainty Budget - Object V9 using worst case estimated uncertainty values.

Contributor	Symbol X_i	Estimated value x_i	unit1	estimated uncertainty	unit2	Probability distribution	divisor	Standard uncertainty $u(x_i)$	sensitivity coefficient c_i	contribution $c_i \cdot u(x_i)$	unit3	contribution (%)
Tilt	X_0	10.1494	cm	8	cm	Rect - R	1.732	4.618938	0.01	0.046189	m	31%
GNSS quality factor	X_1	2.57	cm	2	cm	Normal	1	2	0.01	0.02	m	6%
Tilt error along the sign plane (transverse)	X_2	0	cm	7	cm	R	1.732	4.041570	0.01	0.040416	m	24%
Tilt error perpendicular to the sign plane (longitudinal)	X_3	0	cm	7	cm	R	1.732	4.041570	0.01	0.040416	m	24%
GNSS pole height	X_4	200	cm	1	cm	R	1.732	0.577367	0.01	0.005774	m	0%
Plumb stability error	X_5	0	cm	2	cm	R	1.732	1.154734	0.01	0.011547	m	2%
Centre positioning error (human)	X_6	0	cm	2.5	cm	R	1.732	1.443418	0.01	0.014434	m	3%
Folding scale resolution	X_7	0.1	cm	0.05	cm	R	1.732	0.028868	0.01	0.000289	m	0%
Folding scale measurement error	X_8	0	cm	2	cm	R	1.732	1.154734	0.01	0.011547	m	2%
Object instability error	X_9	0	cm	3	cm	R	1.732	1.732102	0.01	0.017321	m	4%
Pole edge to sign offset	X_{10}	0	cm	2	cm	R	1.732	1.154734	0.01	0.011547	m	2%
Pole centre to measurement point	X_{11}	2.5	cm	2	cm	R	1.732	1.154734	0.01	0.011547	m	2%
									combined standard measurement uncertainty u_c	**0.082918**		**100%**

Table 3.3: Uncertainty Budget - Object V13 using Trafikverket defined limits for estimated uncertainties.

Contributor	Symbol X_i	Estimated value x_i	unit1	estimated uncertainty	unit2	Probability distribution	divisor	Standard uncertainty $u(x_i)$	sensitivity coefficient c_i	contribution $c_i \cdot u(x_i)$	unit3	contribution (%)
Tilt	X_0	137.3496	cm	8	cm	Rect - R	1.732	4.618938	0.01	0.046189	m	32%
GNSS quality factor	X_1	3.16	cm	3	cm	Normal	1	3	0.01	0.03	m	14%
Tilt error along the sign plane (transverse)	X_2	0	cm	6	cm	R	1.732	3.464203	0.01	0.034642	m	18%
Tilt error perpendicular to the sign plane (longitudinal)	X_3	0	cm	6	cm	R	1.732	3.464203	0.01	0.034642	m	18%
GNSS pole height	X_4	200	cm	0.5	cm	R	1.732	0.288684	0.01	0.002887	m	0%
Plumb stability error	X_5	0	cm	2	cm	R	1.732	1.154734	0.01	0.011547	m	2%
Centre positioning error (human)	X_6	0	cm	3	cm	R	1.732	1.732102	0.01	0.017321	m	5%
Folding scale resolution	X_7	0.1	cm	0.05	cm	R	1.732	0.028868	0.01	0.000289	m	0%
Folding scale measurement error	X_8	0	cm	2	cm	R	1.732	1.154734	0.01	0.011547	m	2%
Object instability error	X_9	0	cm	2.5	cm	R	1.732	1.443418	0.01	0.014434	m	3%
Pole edge to sign offset	X_{10}	0	cm	3	cm	R	1.732	1.732102	0.01	0.017321	m	5%
Pole centre to measurement point	X_{11}	2.5	cm	2	cm	R	1.732	1.154734	0.01	0.011547	m	2%
									combined standard measurement uncertainty u_c	**0.081550**		**100%**

Table 3.4: Uncertainty Budget - Object V23 using nominal values for the estimated uncertainty.

The custom-made reference object is designed and manufactured in RISE. The object is a truss mast on a concrete fundament. Once the set up was completed, data collection was initiated. The road sign classification was approached from a different direction, based on their stability and type. A brief classification consisting on three main classes and multiple subclasses is built, but it is not complete. The future work can help define it much clearer. The field measurements on road signs were conducted using a standard measurement pole mounted with a GNSS land surveyor. A total of 27 measurements were completed and a handful of them turned out to be tilting greater than 7°. The object V9 shown in Fig xxx has the highest tilt, and is chosen for the uncertainty analysis. The measurement uncertainty factors were chosen carefully, and the budget was built. From the budget, it can be observed that the error in measuring the tilt in longitudinal and lateral direction had the biggest influence on the measured tilt. The object was moving quite a lot in both the planes and the inability to determine its resting position were the main causes.

4

Results and conclusions

In this section, there are three parts. The initial observations that were made upon inspecting the road signs on the streets of Gothenburg, and after contacting the companies responsible for providing the road signs and maintaining them. Some preliminary conclusions were drawn from the observations. Next section talks about the field work, i.e., the road sign measurements performed on the Astazero test track, and the uncertainty analysis performed on it. The last section explains the results obtained from the anchor point (custom-made reference object), the observations made and the conclusions drawn from it by comparing the performance with regular road signs.

4.1 Initial observations

Upon walking around the city of Gothenburg, observing and gently shaking the road signs, it was seen that generally road signs are not as stable as expected. They do not always meet the standards associated, be it the size of the pole or it's placement. A large percentage of them are shaky and can be taken down without much effort. A lot of signs were also uprooted on the streets, due to various factors like loose soil, vandalism, vehicle crashing into them, roadworks, etc. This led to performing an analysis of the road signs on the Astazero track.

4.2 Field work

After the measurement of the road signs, the data obtained was cleaned and processed using MATLAB. During the process, the dataset was visualised.

Fig 4.1 gives us the GPS positions of the objects along the Astazero track. The track GPS position data helped to check the validity of the road-sign position data collected. A total of 27 objects were recorded on one side of the track, when traversed in clockwise direction.

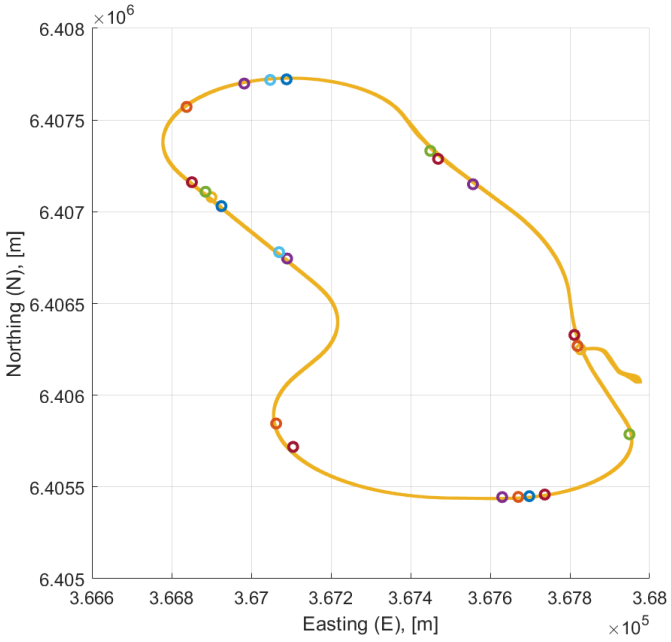

Figure 4.1: SWEREF 99 TM positions plot of various objects along the Astazero track.

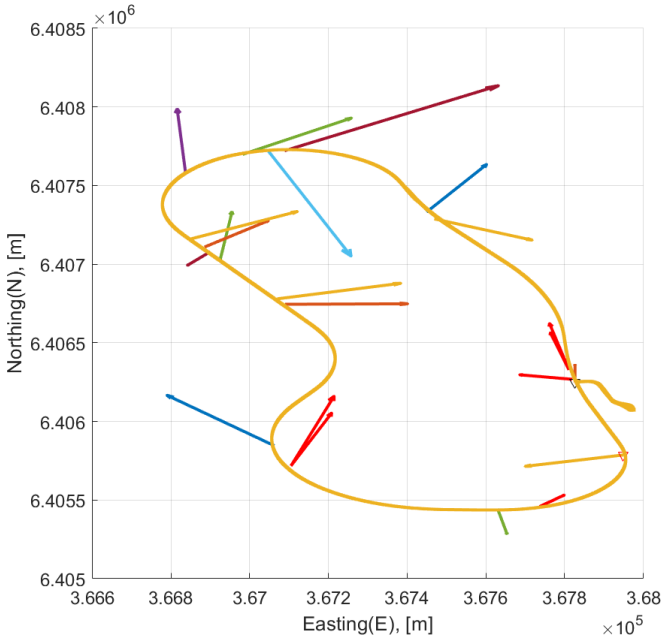

Figure 4.2: Vector plot showing the heading arrows of all the road signs measured along one side of the track.

Fig 4.2 shows the heading arrow of each road sign. The whole dataset was processed, and histograms plotted for the same. The heading angle of the poles (Fig. 4.3) shows that despite experiencing similar weather, winds, soil characteristics, etc., there seems to be no common pattern in which the signs are heading. On the other

hand, The tilt angle histogram shown in Fig. 4.4 can help understand that most of the poles are vertical standing and a mere five out of the twenty seven objects have a tilt greater than 7°.

The worst case scenario in terms of tilting is shown in Fig 3.8. This road signs was at the side of a merging point where a secondary road merged into a main road. It was placed quite far from the road, with low chances of interaction with humans or other vehicles. Despite being undisturbed by these factors, it had tilted considerably. This kind of uncertainty associated with the reliability of the road signs can help conclude that road signs cannot be used as long-term reference objects for autonomous driving, as they are.

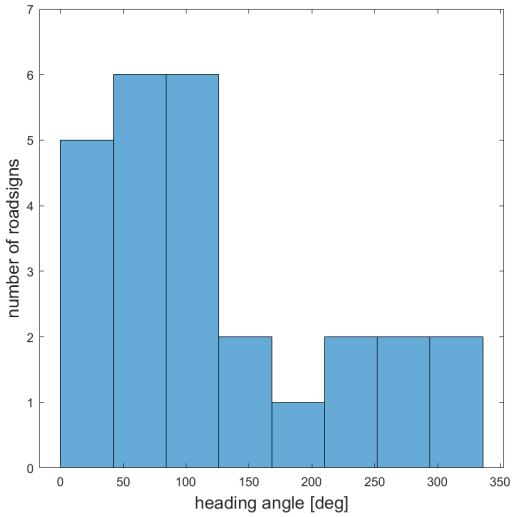

Figure 4.3: Heading angle histogram.

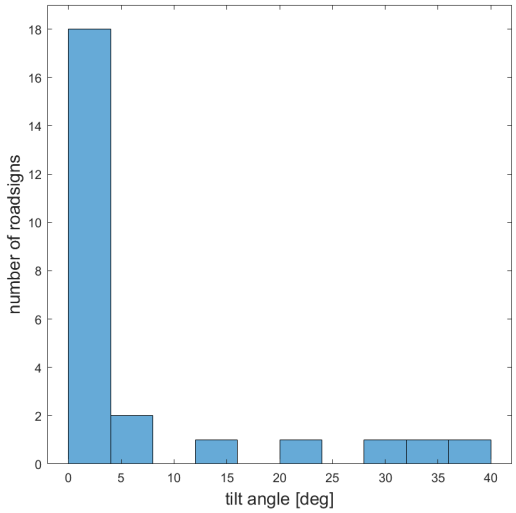

Figure 4.4: Tilt angle histogram.

After that, uncertainty budgets were constructed for three cases, and the case mentioned in Table 3.2 was studied in detail, since it was for the worst-case object. From the results, it can be observed that the tilt itself has some uncertainty associated with it. While placing the measurement pole at the centre of the sign pole, the error in the transverse and longitudinal plane contributes significantly towards the combined uncertainty. From this, it can be said that the stability of the object influences the point of measurement, i.e., if the sign pole wobbles with the wind, one cannot find the default resting position of the road sign (since there is none), and then project the exact point of the road sign's centre on the ground using a plumb.

4.3 Custom-made reference object

After the anchor point was set up, continuous data collection was initiated. The data set used in the thesis was collected between 06-05-2022 till 25-06-2022. The mean μ (E, N and H GNSS co-ordinates) and standard deviation σ (E, N and H GNSS co-ordinates) values were calculated from the data set to be (3.6766×10^5, 6.4070×10^6, 194.1583) m and (0.0051, 0.0064, 0.0145) m, respectively. The height values indicated represent the height above the sea level.

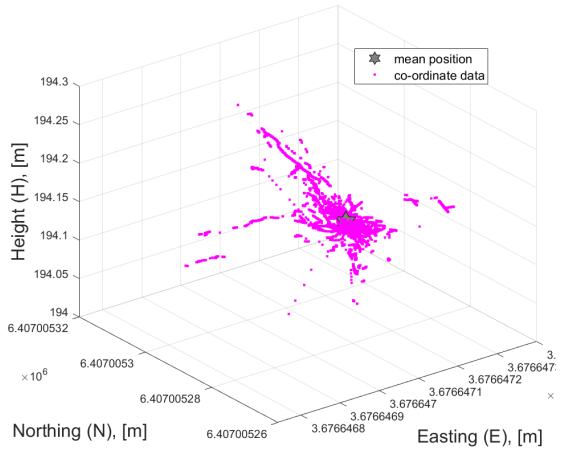

Figure 4.5: 3D plot of SWEREF 99 TM co-ordinates with mean position.

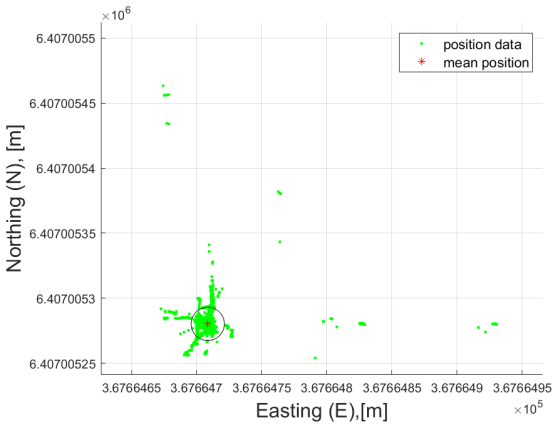

Figure 4.6: SWEREF 99 TM co-ordinates along with the mean and 2σ circle.

Fig. 4.5 show the 3D position of the anchor point (custom-made reference object) over time, recorded by the GNSS receiver. The 2σ standard deviation circle in Fig. 4.6 shows that a majority of the data lies within the limit. The points which lie outside the standard deviation circle may be due to a variety of factors ranging from environmental/weather conditions to wildlife blocking the antenna.

The weather conditions recorded by the weather station was unsatisfactory. There was lot of data losses, and hence, the forecasted weather data was utilised for this thesis, in order to draw conclusions.

Out of 126,707 data points, a mere 6,146 points are beyond the 2σ standard deviation limit. This shows that the object has been quite stable over the period when the data was collected.

In Fig. 4.9, 4.8 and 4.7 are histograms of each component that agree with the result. The majority of the dataset is lying around the mean of the normally distributed data, which shows that the average position of the anchor point changed only by a small extent over a month.

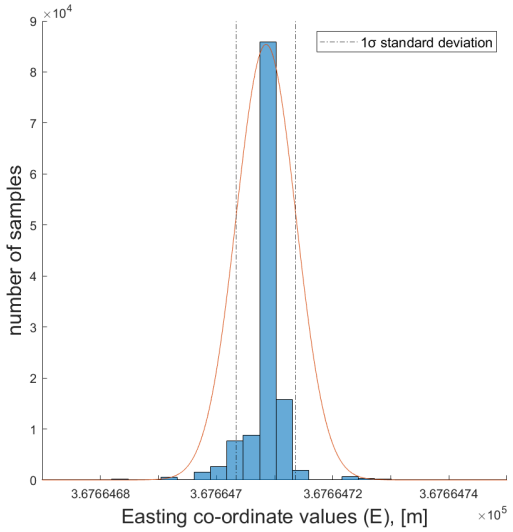

Figure 4.7: The histogram of the Easting co-ordinate samples.

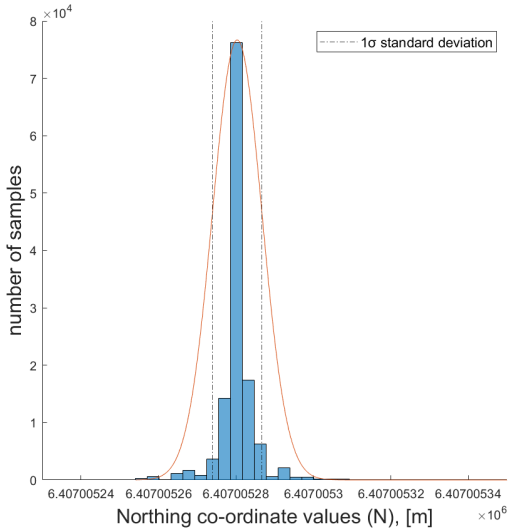

Figure 4.8: The histogram of the Northing co-ordinate samples.

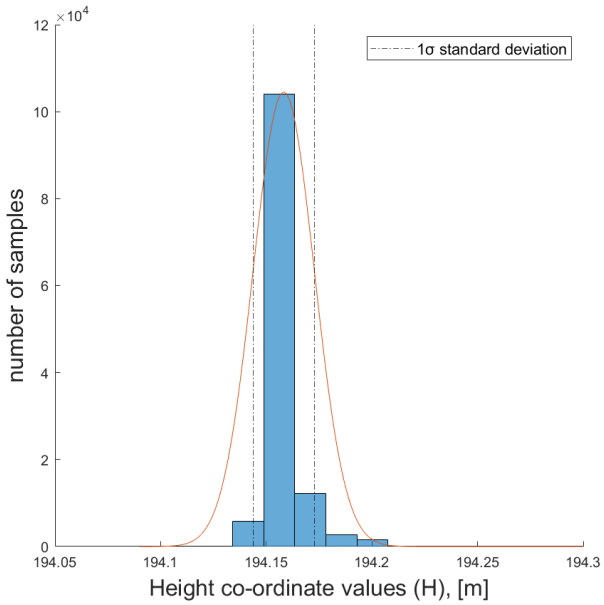

Figure 4.9: The histogram of the Height co-ordinate samples.

When we plot the difference between the position and the mean value μ, it can be observed again from Fig. 4.10 that the position over time is almost a straight line, with small amount of deviations, further supporting the result.

The small peak is observed between the 20000^{th} and 40000^{th} sample because of the data error during one of the days, leading to the usage of an alternative processing solution. The script used to process the large dataset into a single file uses a backward and forward continuity check, and it was observed that between days, the data integration was not seamless as expected. This error also causes some outliers

in the data in the beginning/end of each day.

The major error occurs between the 60,000th and 80,000th sample, and this could probably be caused by birds covering the receiving antenna and hence reducing the effective area, or very bad weather that led to an error in recording.

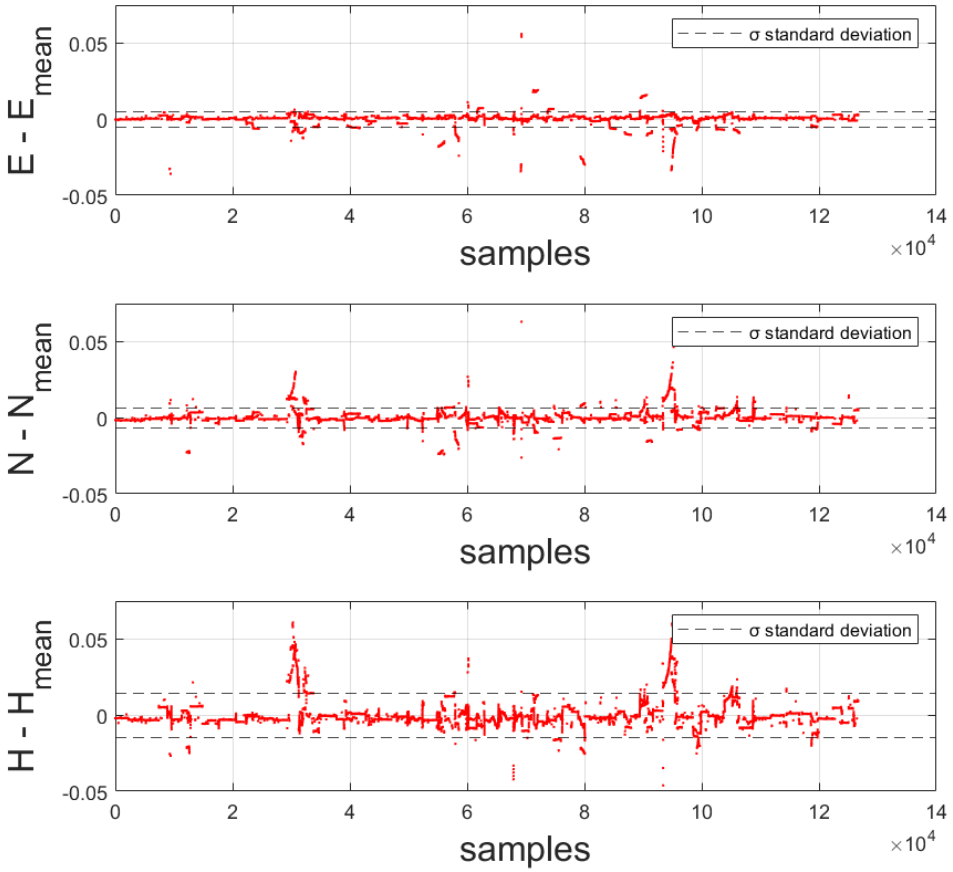

Figure 4.10: The plots for the co-ordinates - mean value (x_i - μ) in all three dimensions.

After visualising the data, an uncertainty budget was constructed for the mean GNSS position as shown in Table 4.1.

4.4 Uncertainty analysis - anchor point

4.4.1 The mean GPS position (N) X_1

This is the mean of the SWEREF 99 TM co-ordinate data collected by the GNSS receiver setup incorporated on the custom-made truss mast in Astazero track. The estimated value used in this budget is the mean value of the Northing co-ordinates recorded and the uncertainty associated with it is the standard deviation of the same.

The reason for using the northing co-ordinate was because it was the direction with the highest standard deviation value. A normal distribution has been used since the data exhibits a symmetry around the mean value when plotted as a histogram.

4.4.2 The height of the GNSS receiver from ground X_2

This is the height of the receiving antenna mounted on the truss mast, from the ground level. It is included to correct any uncertainties while measuring the height. A rectangular distribution is chosen because there is an equal probability of having every value between zero and the estimated uncertainty.

4.4.3 The post processing error X_3

During some days within the data collection period, the data was in a different format from others. This variation made it harder to compile data one day to another. This factor is included to make up for the small discontinuity that is associated with the method employed to compile multiple days of data into a single file.

A rectangular distibution is used for this since the amount of error produced is random and all values within the range are equally probable.

4.4.4 The object tilt error X_4

This factor is used to correct any uncertainties produced during the measurement of the truss mast tilt. The tool used for this was an analog spirit level.

A rectangular distribution is utilized since there was no difference observed in the measurement when it was repeated in the same direction.

4.4.5 The soil setting/sinking error X_5

Soil sinks over time due to geological phenomena and forces acting on it. This effect is corrected by introducing a factor X_5.

A rectangular distribution is used here.

4.4.6 The error due to the thermal expansion of the steel mount X_6

This factor is used to correct the expansion and contraction of the steel truss mast due to extreme temperatures experienced annually. The linear thermal expansion was calculated using the equation:

$$\Delta L = \alpha L \Delta T \tag{4.1}$$

where ΔL is the change in length of object, α is the thermal expansion co-efficient (for steel = (10 to 13)$\times 10^6$ K^{-1}).

4.4.7 The centre positioning error (human) X_7

This factor compensates for the uncertainty introduced by human eyes while trying to determine object centre using the folding rule.

The distribution employed for this is rectangular, since the chance of the uncertainty tipping towards either side of the measurement has an equal probability.

4.4.8 The folding scale resolution X_8

This factor is similar to the one used in Table 3.2, compensating for the uncertainty introduced due to the least count of a folding rule which may go unnoticed by the human eye. The same distribution as previously is used.

4.4.9 The folding scale measurement error X_9

This factor is also common to both budgets, which compensates for the errors produced when a human repeats a measurement.

It uses a rectangular distribution since the probability of the estimated uncertainty varying between the limits is equal.

4.4.10 The object instability error X_{10}

This factor is introduced to compensate for any instability that may be produced in the object due to the heavy fundament slowly displacing in the soil.

A rectangular distribution is employed since there's a uniform probability of occurrence of all variables within the dataset.

4.4.11 The heavy vehicle vibrations causing temporary disruptions X_{11}

This error was introduced to compensate for the small displacement of the object due to vibrations caused by fully loaded heavy vehicles moving on structures such as bridges, etc, or when some roadwork/construction is carried out around it.

A rectangular distribution is utilised for this.

Contributor	Symbol X_i	Estimated value x_i	Unit1	Estimated uncertainty	Unit2	Probability distribution	Divisor	Standard uncertainty $u(x_i)$	Sensitivity co-effiecient c_i	Contribution $c_i \cdot u(x_i)$	Unit4	Contribution (%)
Mean GPS position (N)	X_0	640700528.032685	cm	0.8	cm	Normal	1	0.8	0.01	0.008	m	8%
Height of GNSS receiver from ground	X_1	350	cm	2	cm	Rect - R	1.732	1.154734	0.01	0.011547	m	18%
Post processing errors	X_2	0	cm	1.5	cm	R	1.732	0.866051	0.01	0.008661	m	10%
Object tilt error	X_3	0	cm	0.5	cm	R	1.732	0.288684	0.01	0.002887	m	1%
Soil setting or sinking	X_4	0	cm	1	cm	R	1.732	0.577367	0.01	0.005774	m	4%
Thermal expansion of the truss mast	X_5	0	cm	0.195	cm	R	1.732	0.112587	0.01	0.001126	m	0%
Center positioning error (human)	X_6	0	cm	3	cm	R	1.732	1.732102	0.01	0.017321	m	40%
folding scale resolution	X_7	0	cm	0.05	cm	R	1.732	0.028868	0.01	0.000289	m	0%
folding scale measurement error	X_8	0	cm	2	cm	R	1.732	1.154734	0.01	0.011547	m	18%
object instability error	X_9	0	cm	0.1	cm	R	1.732	0.057737	0.01	0.000577	m	0%
Vibration from heavy vehicles nearby	X_{10}	0	cm	0.5	cm	R	1.732	0.288684	0.01	0.002887	m	1%
								Combined standard measurment uncertainty u_c		**0.027521**		**100%**

Table 4.1: Uncertainty budget for the anchor point

The visualisation results show that the overall short-term stability of the object is pretty good. The variation of the position is very small, and most of the time lies within the σ limits. The outliers are due to the integration errors during post-processing, foreign objects obstructing the antenna (like birds), extreme weather conditions, etc.

Upon comparison, it can be clearly observed that the custom-made anchor point is much stronger structurally, more stable and hence has a much higher possibility of being used as a long-term reference object. The overall combined standard measurement uncertainty is also much smaller than that associated with the regular road signs, as the object is more stable and easier to perform measurements than the road signs.

4.5 Summary

From the initial observations, it could be seen that trafikverket does not directly play a huge role in maintaining the road sign standards. It is assigned to third party companies. These companies are provided with the set of rules to be followed but the adherence is okay at best. The suppliers and the manufacturers have no contact with each other. Prioritising traceability can help improve the maintenance and accountability.

From the road signs, it was observed that seven out of twenty seven signs lean more than 5°, and when an uncertainty analysis was performed on the worst case, it has a large combined standard measurement uncertainty value. The road signs inside the test track had similar, but slightly better maintenance standards.

From the final section, after analysis and building the uncertainty budget, comparing the combined standard measurement uncertainty value with the regular road sign, it can be clearly said that the custom object has higher reliaiity and lesser uncertainty associated eith it. The object also delivers the Class 2A performance as expected.

Furthermore, only the GNSS position values were used in this thesis. A clearer idea can be obtained upon mounting the prisms on the mast and taking laser scanner measurements.

5

Discussions and future scope

The study conducted on the road signs and observing road signs on a regular basis has provided lot of insights. They are listed below:

- The standards defined for road signs can be quite confusing, hence organising workshops in order to spread the awareness about them, and clearing doubts that arise can increase the efficiency and standard compliance of the companies who are manufacturing, planting, and maintaining the road signs.
- The stability of the road sign is affected by multiple factors such as its light weight and hollow pole, the type of soil in which it is placed, the settlement characteristics of the soil, the placement angle, the wind speeds, the fundament type, and many other factors.
- Road signs can be easily meddled with, hence periodic checks by the trafikverket for vandalism, tilting and uprooting can help make the road safer, along with increasing the reliability of the sign in case they are planned to be used as a temporary reference.
- During the literature study, it was found that the traceability of a road sign from its manufacturing phase to after a few years of its usage is very bad. The agencies that supply the signs, plant the signs, and the ones who maintain the signs lack communication among themselves. Upon contacting these agencies, none of the contact persons had any information regarding the standards they follow.

While building the uncertainty table, a few things were noted, in order to refine it further. For example, the variable x_{10} in Table 3.2 is the pole edge to sign offset. This variable uncertainty can increase or decrease depending on the location on the pole at which the measurement is made. If the measurement is performed on the pole in the same side as the sign, the value is small, whereas when the measurement is taken in the opposite direction, or at the sides of the pole, the uncertainty varies. This uncertainty can be eliminated by deciding a standard point at which the measurement is made, and following the same procedure for all the trials performed on all the objects.

Since the anchor point was only ready for installation in the later part of the project, long term study could not be performed on it. A future scope of this project would be to obtain more data, and observe how it fares in the long term.

As of now, the anchor point is only recording GNSS data. Once the magnetic ball base is installed, geodetic measurements using total stations and laser scans can be

performed, increasing the volume of data to be analysed. This will help study the stability and the anchor point's potential to be a reference object.

Since the weather station used in Astazero was not completely reliable at all times, implementing a weather station for the purpose of the project would help better understand the impact of weather on the anchor point.

The impact of the strong coastal winds and the annually occurring frost and thaw cycles on the stability and tilt of the sign can be studied in detail, while establishing a relationship between the anchor point and the road sign attached to it, since the current study only focuses on the stability of the anchor point itself and not the road sign mounted on the truss mast.

As already stated, foreign objects such as birds can block the receiving antenna. There have been studies performed in order to determine the effect of bird visits on SWEPOS stations. One solution studied by RISE was the utilization of radomes [28]. Radomes are structures which provide weather-proofing and intruder proofing via a dome, within which the receiving RADAR antenna is placed. The radomw is usually made of plastic or acrylic textile based materials, and chosen carefully such that the frequencies of communication between the receiving antenna and the received signals can pass through the dome without considerable losses. The radomes are manufactured by blow moulding compressed air bubbles on a sheet of the chosen material. The receiving system is either calibrated after radome installation, or the losses due to the dome are corrected for. Detrmining the best type of radome for the purpose, its incorporation in the system, and the performance measurement of the anchor point can also be performed in the future.

5.1 Ethical and sustainability aspects of the thesis

All the uncertainty factors represented in the budgets are slightly exaggerated in order to maintain a small safety margin while determining the stability of the objects to account for any other unexpected factors.

Determining and understanding the stability of road signs helps decide better about how the sign boards can be used to guide autonomous vehicles with lower positioning uncertainty, and to get an idea of how these objects can be improved based on the factors that influence the measurement uncertainty. This will help ADAS and CV applications achieve higher accuracy, and the manufacturers and governments to move closer to achieving the goals of **Vision Zero** [12] by making the HD maps more detailed while reducing the positioning errors caused during autonomous driving. It will also help reduce the effort involved in the driving task, reducing the mental stress of the driver while allowing them to perform secondary tasks in the future. Once the existing roadside infrastructure is improved to provide lower positioning uncertainty, they can be used as references, saving resources on producing new ones making the idea sustainable.

From the observations, it was concluded that the maintenance of the road signs could

be better. The results of this project can help the road transport organisations to build more sustainable and stronger road signs, and find novel ways for their maintenance. One such idea would be to involve the public via a mobile application to identify the broken/vandalised road sign poles, upload a picture and describe the problem, so that the ones which need immediate attention can be fixed sooner.

When vehicles are connected via wireless networks for communication, a lot of energy and resources are utilised which might increase the carbon footprint, but this can be justified by the improved traffic situation and passenger safety while improving the positioning accuracy.

Bibliography

[1] N. Williams and M. Barth, "A qualitative analysis of vehicle positioning requirements for connected vehicle applications," *IEEE Intelligent Transportation Systems Magazine*, vol. 13, no. 1, pp. 225–242, 2020.

[2] A. Zang, Z. Li, D. Doria, and G. Trajcevski, "Accurate vehicle self-localization in high definition map dataset," in *Proceedings of the 1st ACM SIGSPATIAL Workshop on High-Precision Maps and Intelligent Applications for Autonomous Vehicles*, pp. 1–8, 2017.

[3] M. Hirabayashi, A. Sujiwo, A. Monrroy, S. Kato, and M. Edahiro, "Traffic light recognition using high-definition map features," *Robotics and Autonomous Systems*, vol. 111, pp. 62–72, 2019.

[4] F. Li, P. Bonnifait, J. Ibanez-Guzman, and C. Zinoune, "Lane-level map-matching with integrity on high-definition maps," in *2017 IEEE Intelligent Vehicles Symposium (IV)*, pp. 1176–1181, IEEE, 2017.

[5] J. Bjelfvenstam, "Vägen till självkörande fordon - introduktion." https://www.regeringen.se/rattsliga-dokument/statens-offentliga-utredningar/2018/03/vagen-till-sjalvkorande-fordon---introduktion/, March 2018. Accessed: 06-05-2022.

[6] P. Medici, C. Caraffi, E. Cardarelli, P. P. Porta, and G. Ghisio, "Real time road signs classification," in *2008 IEEE International Conference on Vehicular Electronics and Safety*, pp. 253–258, IEEE, 2008.

[7] A. Broggi, P. Cerri, P. Medici, P. P. Porta, and G. Ghisio, "Real time road signs recognition," in *2007 IEEE Intelligent Vehicles Symposium*, pp. 981–986, IEEE, 2007.

[8] G. K. Siogkas and E. S. Dermatas, "Detection, tracking and classification of road signs in adverse conditions," in *MELECON 2006-2006 IEEE Mediterranean Electrotechnical Conference*, pp. 537–540, IEEE, 2006.

[9] I. BIPM, I. IFCC, I. IUPAC, and O. ISO, "The international vocabulary of metrology—basic and general concepts and associated terms (vim), 3rd edn. jcgm 200: 2012," 2012.

[10] "International vocabulary of legal metrology (VIML)," vol. 1, pp. 16–17, International organisation of legal metrology (OIML), 2013.

[11] "European commission welcomes launch of global plan for the UN decade of action on road safety 2021-2030." shorturl.at/gnAK9, October 2021. Accessed: 27-04-2022.

[12] "A primer on vision zero: Advancing safe mobility for all." https://visionzeronetwork.org/wp-content/uploads/2018/05/What-is-VZ_FINAL.pdf, October 2021. Accessed: 16-02-2022.

[13] J. Jiao, "Machine learning assisted high-definition map creation," in *2018 IEEE 42nd Annual Computer Software and Applications Conference (COMPSAC)*, vol. 1, pp. 367–373, IEEE, 2018.

[14] "GNSS frequency band." https://www.rfwireless-world.com/Terminology/GPS-Frequency-Band-and-GNSS-Frequency-Band.html?msclkid=462795ddd12a11ec9308d0e498b03b4c, 2016. Accessed: 11-05-2022.

[15] "International GNSS service." https://igs.org/. Accessed: 08-08-2022.

[16] T. Soler and L. D. Hothem, "Coordinate systems used in geodesy: Basic definitions and concepts," *Journal of surveying engineering*, vol. 114, no. 2, pp. 84–97, 1988.

[17] "SWEREF 99." https://www.lantmateriet.se/en/maps-and-geographic-information/gps-geodesi-och-swepos/reference-systems/three-dimensional-systems/SWEREF-99/, 2021. Accessed: 25-04-2022.

[18] T. Kempe, A. Alfredsson, B. Andersson, L. E. Engberg, F. Dahlström, and G. Lohász, "The process of changing from local systems into sweref 99,"

[19] T. Kempe and J. Ågren, "Om SWEN17_RH2000 - den nya nationella geoidmodellen," *Sveriges Kart- Mätningstekniska Förenings*, vol. 1, no. 12-13, 2019.

[20] K. C. Wang, Z. Hou, and W. Gong, "Automated road sign inventory system based on stereo vision and tracking," *Computer-Aided Civil and Infrastructure Engineering*, vol. 25, no. 6, pp. 468–477, 2010.

[21] L. Hazelhoff, I. M. Creusen, and P. H. De With, "Optimal performance-efficiency trade-off for bag of words classification of road signs," in *2014 22nd International Conference on Pattern Recognition*, pp. 2996–3001, IEEE, 2014.

[22] A. Broggi, P. Cerri, P. Medici, P. P. Porta, and G. Ghisio, "Real time road signs recognition," in *2007 IEEE Intelligent Vehicles Symposium*, pp. 981–986, IEEE, 2007.

[23] S. Hamdi, H. Faiedh, C. Souani, and K. Besbes, "Road signs classification by ann for real-time implementation," in *2017 International Conference on Control, Automation and Diagnosis (ICCAD)*, pp. 328–332, IEEE, 2017.

[24] A. Adam and C. Ioannidis, "Automatic road-sign detection and classification based on support vector machines and hog descriptors.," *ISPRS Annals of Photogrammetry, Remote Sensing & Spatial Information Sciences*, vol. 2, no. 5, 2014.

[25] F. Paiva and R. C. Barros, "Analysis of the stability and design of cantilevered sign supports in highways," in *Madeira Conference: Integrity, Reliability and Failure of Mechanical Systems*, 2013.

[26] A. Namdar, Y. Dong, and Y. Deyu, "The effect of concrete footing shape in differential settlement: A seismic design," *Advances in Civil Engineering*, 2019.

[27] B. Eklund and U. Påhlsson, *Handbok VägmärkenVägverkets strategiska inriktning för kommunikation*. Vägverket, 2009.

[28] J. Johansson, M. Lidberg, P. Jarlemark, K. Ohlsson, J. Löfgren, L. Jivall, and T. Ning, "Close-rtk 3: High-performance real-timegnss services," 2019.

DEPARTMENT OF SOME SUBJECT OR TECHNOLOGY
CHALMERS UNIVERSITY OF TECHNOLOGY
Gothenburg, Sweden
www.chalmers.se

CHALMERS
UNIVERSITY OF TECHNOLOGY